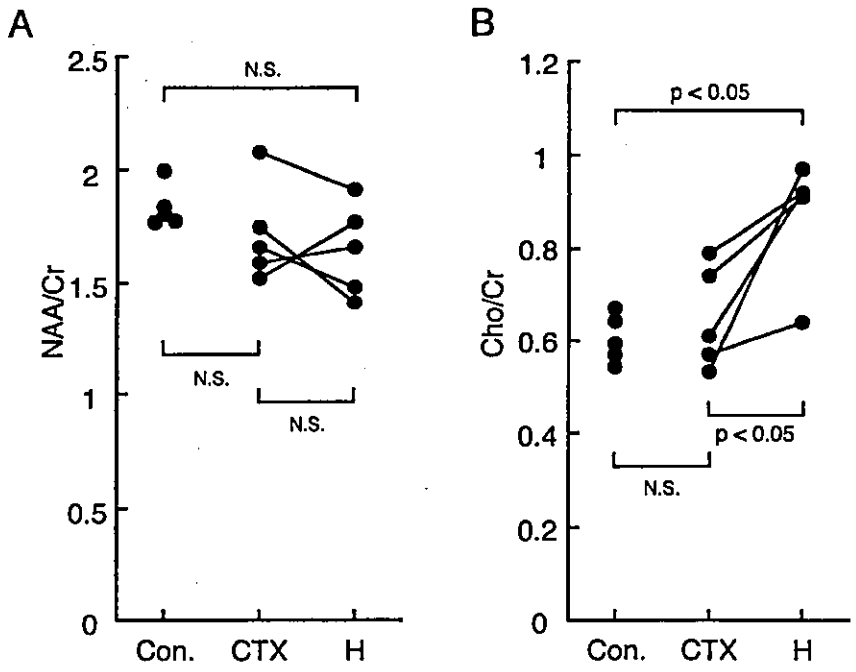

FIG. 4. The summarized ^{1}H-magnetic resonance spectroscopy (MRS) results for the band heterotopia patients. A: *N*-acetyl aspartate (NAA)/creatinine (Cr) ratio in the cortex of a normal volunteer (Con.), in the external normal cortex of the patients (CTX), and in the laminar heterotopia (H). There were no significant differences in the NAA/Cr among Con., CTX, and H. B: The choline (Cho)/Cr ratio in CD and Con. The Cho/Cr ratio was significantly higher in H ($p < 0.05$), whereas no significant difference was seen between Con. and CTX. Lines connect the data from the same patient. N.S., no significant difference.

tends to be highest in very young infants (15); therefore the increased Cho/Cr ratio in the CD lesions suggests that there is increased membrane turnover and tissue immaturity. A previous article reported that the Cho signal is decreased in the CD area (18). Although the reason for this discrepancy remains unknown, a possible explanation may lie in the difference in the age of the patients. In our study, the patients with CD were younger than those in the previous report (18). The Cho level in CD might change with age, presumably in a manner different from that of the normal brain. Further study is required to clarify the metabolic differences between other CDMs and to assess age-dependent changes in the MRS signal of CD lesions.

BH is characterized by a laminar heterotopia that is mainly caused by mutations in the *doublecortin* gene in Xq22.3 (21). Histologically, the external cortex appears nearly normal, with the usual six layers (5). The heterotopic band consists of morphologically differentiated pyramidal cells that are randomly arranged (5). Fluorodeoxyglucose positron emission tomography (PET) and single-photon emission computed tomography (SPECT) findings showed similar glucose metabolism and blood flow in the heterotopic band and normal external cortex (22), whereas these studies showed variably abnormal patterns in other CDMs (22,23). These histologic and functional findings imply fewer metabolic abnormalities in BH than in other CDMs. Our study revealed that the NAA/Cr ratio of the laminar heterotopia did not significantly differ from that of the external cortex in BH or of the normal cortex of volunteers. Previous studies have shown that the NAA signal from subcortical heterotopia ranges from normal to below normal, suggesting that the maturity differs from case to case (17). A few cases of BH have had a normal or slightly decreased NAA signal (6,17). A recent functional MRI study reported that finger tapping activated both the normal sensorimotor cortex and the laminar heterotopia facing it, suggesting that the laminar heterotopia of BH has specific synaptic connections with the external cortex (6,7). Synaptic stimulation may facilitate neuronal differentiation in BH (24). By contrast, the Cho/Cr signal was significantly higher in the heterotopic area than in the cortex. The intense Cho signal may result from unusual Cho turnover. Another possible explanation is the presence of bundles of myelinated fibers projecting from the neocortex to remote brain areas, which pass through the laminar heterotopia (5). As shown in MRS spectra of the white matter, myelinated fibers have a relatively intense Cho signal (15); therefore these fibers may enhance the Cho signal from the laminar heterotopia.

This study revealed that the ^{1}H-MRS signals of BH were relatively normal, suggesting that neurons in the heterotopic tissue of BH are relatively well differentiated. However, BH is often associated with intractable epilepsy, although the motor and mental impairment in BH is less severe than in other diffuse CDMs. Therefore the results of MRS do not predict the severity of the epilepsy in BH. In CD patients, there also was no obvious correlation between the metabolite ratios and the severity of the neurologic symptoms, as in previous reports (16–18); therefore the MRS data are thought to

correlate more with developmental abnormalities or tissue disorganization than with the clinical severity of the disease in the patients.

The tissue of CD consists of abnormally developed cells and is highly epileptogenic (19,25). By contrast, the heterotopic neurons in BH are relatively differentiated; consequently, the mechanism for the epileptogenicity of BH might be distinct from that of CD. Interestingly, in the *tish* rat, an epileptic model rat for band heterotopia, the heterotopic neurons have aberrant connections with neurons in the external cortex (26), and the external cortex is responsible for initiating the seizure discharges in heterotopic tissue (27). In BH patients, intraoperative electrocorticography with a deep electrode showed that clinical seizures arise in the external cortex, whereas electrical activity in heterotopia does not produce clinical seizures directly (28). Focal surgical removal of the putative epileptogenic tissue in BH patients produces inadequate results, even in the presence of a localized epileptogenic area (28). These experimental and clinical reports suggest that epileptic activity is not simply generated within the heterotopic tissue. The abnormal neuronal network formed by the heterotopic neurons might be responsible for the epileptogenicity in BH. Further investigation is required to clarify the mechanism of epileptogenicity in BH.

REFERENCES

1. Aicardi J. The agyria-pachygyria complex: a spectrum of cortical malformations. *Brain Dev* 1991;13:1–8.
2. Kuzniecky RI, Barkovich AJ. Malformations of cortical development and epilepsy. *Brain Dev* 2001;23:2–11.
3. Dobyns WB, Truwit CL. Lissencephaly and other malformations of cortical development: 1995 update. *Neuropediatrics* 1995; 26:132–47.
4. Kuzniecky RI. Neuroimaging in pediatric epilepsy. *Epilepsia* 1996;37(suppl 1):S10–21.
5. Harding B. Gray matter heterotopia. In: Guerrini R, Andermann F, Canapicchi R, eds. *Dysplasia of cerebral cortex and epilepsy.* Philadelphia: Lippincott-Raven, 1996:81–8.
6. Iannetti P, Spalice A, Raucci U, et al. Functional neuroradiologic investigations in band heterotopia. Pediatr Neurol 2001;24:159–63.
7. Pinard J, Feydy A, Carlier R, et al. Functional MRI in double cortex: functionality of heterotopia. *Neurology* 2000;54:1531–3.
8. Robain O. Introduction to the pathology of cerebral cortical dysplasia. In: Guerrini R, Andermann F, Canapicchi R, eds. *Dysplasia of cerebral cortex and epilepsy.* Philadelphia: Lippincott-Raven, 1996:1–9.
9. Spreafico R, Battaglia G, Arcelli P, et al. Cortical dysplasia: an immunocytochemical study of three patients. *Neurology* 1998;50: 27–36.
10. Novotny E, Ashwal S, Shevell M. Proton magnetic resonance spectroscopy: an emerging technology in pediatric neurology research. *Pediatr Res* 1998;44:1–10.
11. Castillo M, Kwock L, Mukherji SK. Clinical applications of proton MR spectroscopy. *AJNR Am J Neuroradiol* 1996;17:1–15.
12. Whiting S, Duchowny M. Clinical spectrum of cortical dysplasia in childhood: diagnosis and treatment issues. *J Child Neurol* 1999; 14:759–71.
13. Caraballo R, Cersosimo R, Fejerman N. A particular type of epilepsy in children with congenital hemiparesis associated with unilateral polymicrogyria. *Epilepsia* 1999;40:865–71.
14. Pascual-Castroviejo I, Pascual-Pascual SI, Viano J, et al. Unilateral polymicrogyria: a common cause of hemiplegia of prenatal origin. *Brain Dev* 2001;23:216–22.
15. Pouwels PJ, Brockmann K, Kruse B, et al. Regional age dependence of human brain metabolites from infancy to adulthood as detected by quantitative localized proton MRS. *Pediatr Res* 1999; 46:474–85.
16. Kuzniecky R, Hetherington H, Pan J, et al. Proton spectroscopic imaging at 4.1 Tesla in patients with malformations of cortical development and epilepsy. *Neurology* 1997;48:1018–24.
17. Li LM, Cendes F, Bastos AC, et al. Neuronal metabolic dysfunction in patients with cortical developmental malformations: a proton magnetic resonance spectroscopic imaging study. *Neurology* 1998;50:755–9.
18. Simone IL, Federico F, Tortorella C, et al. Metabolic changes in neuronal migration disorders: evaluation by combined MRI and proton MR spectroscopy. *Epilepsia* 1999;40:872–9.
19. Avoli M, Bernasconi A, Mattia D, Olivier A, et al. Epileptiform discharges in the human dysplastic neocortex: *in vitro* physiology and pharmacology. *Ann Neurol* 1999;46:816–26.
20. Hablitz JJ, DeFazio RA. Altered receptor subunit expression in rat neocortical malformations. *Epilepsia* 2000;41(suppl 6):S82–5.
21. Des Portes V, Francis F, Pinard JM, et al. *Doublecortin* is the major gene causing X-linked subcortical laminar heterotopia (SCLH). *Hum Mol Genet* 1998;7:1063–70.
22. Iannetti P, Spalice A, Raucci U, et al. Functional neuroradiologic investigations in band heterotopia. *Pediatr Neurol* 2001;24:159–63.
23. Sasaki K, Ohsawa Y, Sasaki M, et al. Cerebral cortical dysplasia: assessment by MRI and SPECT. *Pediatr Neurol* 2000;23:410–5.
24. Katz LC, Shatz CJ. Synaptic activity and the construction of cortical circuits. *Science* 1996;274:1133–8.
25. Mathern GW, Cepeda C, Hurst RS, et al. Neurons recorded from pediatric epilepsy surgery patients with cortical dysplasia. *Epilepsia* 2000;41(suppl 6):S162–7.
26. Schottler F, Couture D, Rao A, et al. Subcortical connections of normotopic and heterotopic neurons in sensory and motor cortics of the *tish* mutant rat. *J Comp Neurol* 1998;395:29–42.
27. Chen ZF, Schottler F, Bertram E, et al. Distribution and initiation of seizure activity in a rat brain with subcortical band heterotopia. *Epilepsia* 2000;41:493–501.
28. Bernasconi A, Martinez V, Rosa-Neto P, et al. Surgical resection for intractable epilepsy in double cortex syndrome yields inadequate results. *Epilepsia* 2001;42:1124–9.

ELSEVIER

Mitochondrion 3 (2003) 21–27

Mitochondrion

www.elsevier.com/locate/mito

Continuous culture of novel mitochondrial cells lacking nuclei

Kazutoshi Nakano[a,*], Ikuroh Ohsawa[b], Kumi Yamagata[b], Tomohiro Nakayama[a], Kaori Sasaki[a], Mikako Tarashima[a], Kayoko Saito[a], Makiko Osawa[a], Shigeo Ohta[b]

[a]*Department of Pediatrics, Tokyo Women's Medical University, 8-1, Kawada-cho, Shinjuku-ku, Tokyo 162-8666, Japan*
[b]*Department of Biochemistry and Cell Biology, Institute of Gerontology, Nippon Medical School, 1-396, Kosugi-cho, Nakahara-ku, Kawasaki 211-8533, Japan*

Accepted 10 April 2003

Abstract

We isolated stable cell lines, designated as mitochondrial cells, from cybrids obtained by fusing mitochondria-less HeLa cells with platelets from patients with Leigh syndrome, a subtype of mitochondrial encephalomyopathy. The cells contain a pathogenic point mutation, T9176C, in the mitochondrial DNA. Hematoxylin–eosin staining, confocal fluorescent microscopy and flow cytometry in fixed or living cells showed that the majority of these mitochondrial cells lack nuclear DNA and nuclei, but contain active mitochondria. Despite the absence of nuclear DNA, these cells can be continuously generated in culture. Therefore, it is likely that they arise from the minority of cells which possess a nucleus.

Keywords: Mitochondria; Cybrids; Mitochondria-less cells; Leigh syndrome; Nuclei

1. Introduction

Mitochondria have a genome and an expression system separate from those of nuclear DNA. However, only 13 polypeptides are encoded by human mitochondrial DNA (mtDNA). All other mitochondrial proteins are encoded by nuclear genes. Therefore, human mitochondria require nuclear DNA to be maintained. Unlike most other cells, platelets have mitochondria but no nucleus. They are formed by fragmentation of megakaryocytes and they have activity in blood for several days, but have no ability to proliferate.

Human cell lines without mtDNA, designated as Rho^0 cells, were previously isolated (King and Attardi, 1989). These Rho^0 cell lines are useful for investigating the role of mutant mtDNA, as this DNA can be introduced by cytoplasmic transfer. The resultant 'cybrids' have individual mtDNA but a common nucleus, ruling out nuclear background effects. Cell lines obtained by fusing Rho^0 cells with enucleated cells from patients with a variety of mitochondrial diseases have contributed to the understanding of mitochondrial disorders (Chomyn et al., 1992, 1994; Dunbar et al., 1996). This cybrid technique has been widely accepted for analysis of mutant mtDNA. Recently, Schapira and colleagues (Gu et al., 1998)

* Corresponding author. Tel.: +81-3-3353-8111; fax: +81-3-5269-7338.
E-mail address: knakano@ped.twmu.ac.jp (K. Nakano).

1567-7249/03/$20.00
doi:10.1016/S1567-7249(03)00056-4

developed a method of constructing cybrids by fusing platelets with Rho^0 cells for the analysis of Parkinson disease, instead of using enucleated cells as mitochondrial donors.

2. Materials and methods

2.1. Rho^0 cell culture

Human HeLa cell lines depleted of mtDNA (mtDNA-less Rho^0 cells) were cultured in Dulbecco's modified Eagle medium (DMEM; Gibco BRL, USA) supplemented with 10% fetal calf serum, 50 U/ml penicillin, 50 μg/ml streptomycin, 0.2 mM uridine, 2 mM glutamine and 1 mM sodium pyruvate at 37 °C in a humidified gas mixture containing 8% CO_2.

2.2. Platelet preparation

Blood samples were obtained from two siblings with Leigh syndrome, both of whom had a T9176C mutation in the mitochondrial ATPase 6 gene, and two healthy volunteers, a 45-year-old man and a 30-year-old woman. Both volunteers provided informed consent to participate in the study. The siblings were an 18-year-old female and a 13-year-old male whose guardian had agreed to the use of their cells for this research. The clinical details of these cases were reported previously (Makino et al., 1998; Nakano et al., 1999). Platelet isolation was performed within 2 h of obtaining the blood samples, as previously described (Shults et al., 1998).

2.3. Platelet-fused cybrids

Platelet-fused cybrids were obtained by a previously described method (Ohta, 1986). A total of 5×10^7 Rho^0 cells were collected after the addition of 0.05% trypsin–ethylenediaminetetraacetic acid (EDTA), and resuspended in Hank's buffer. The suspension was gently added to the platelet pellet followed by centrifugation at $200 \times g$ for 10 min. The pellet consisted of a mixture of platelets and Rho^0 cells. Two hundred microliters of 0.1% ethyleneglycol in dimethyl sulfoxide (DMSO) were added twice, each time followed by 30 s rest at room temperature. Four milliliters of DMEM without fetal bovine serum (FBS) were then added and gently mixed with the pellet and allowed to stand for 10 min at room temperature. The mixed buffer was added to 40 ml of DMEM with 10% FBS. The cells were cultured in a 96-well plate. Colonies of monoclonal platelet-fused cybrids grew in each well with buffer exchange every 3 days. Monoclonal platelet-fused cybrid cell lines were then established.

2.4. DNA analyses

Genomic DNA was extracted from the cybrids and their derivatives, and from mitochondrial cells derived from the platelets of controls and patients with the T9176C mutation as described by Sambrook et al. (1989). Detection of the T9176C mutation was performed by polymerase chain reaction–restriction fragment length polymorphism (PCR–RFLP) analysis as previously described (Makino et al., 1998; Thyagarajan et al., 1995; Campos et al., 1997). We amplified a 178-bp fragment of mtDNA encompassing the mutation using oligonucleotide primers 5′-GGCCACCTACTCATGCACCTAA-3′, corresponding to mtDNA positions 9025–9046 (forward), and 5′-GTGTTGTCGTGCAGGTAGAGGCTTCCT-3′, corresponding to nt 9203–9177 (reverse), with a T-to-C mismatch at nt 9179, 3 bp from the 3′ end of the primer. The mtDNA nucleotide number was determined as previously described (Anderson et al., 1981). The PCR products were digested with 15 U of ScrfI for 24 h at 37 °C, electrophoresed through a 3% agarose gel and stained with ethidium bromide. In the mutant mtDNA, the mismatch-containing primer introduces a restriction site for ScrfI at nt 9176. Thus, ScrfI cleaves mutant mtDNA into two fragments of 151 and 27 bp, whereas ScrfI does not cut wild type mtDNA and a 178-bp size fragment remains.

2.5. MitoTracker red, MitoTracker green, and SYTO green nucleic acid staining

MitoTracker CMX-Ros probe (hereafter referred to as MitoTracker red) (Molecular Probes, Inc., Oregon) is a lipophilic cationic dye derived from X-rosamine, which is mitochondrion-selective and can be used to measure mitochondrial membrane potential, and is well retained during cell fixation

(Ligon and Steward, 2000). MitoTracker green (Molecular Probes, Inc., Oregon) is also a mitochondrion-selective but membrane potential independent dye (Hollinshead et al., 1997). SYTO green (Syto 16) (Molecular Probes, Inc., Oregon) is a fluorescent dye that stains nucleic acid even in live cells (Frey, 1995). After adding 20 nM MitoTracker red and 100 nM MitoTracker green or 1 μM SYTO green, the samples were left standing for 15 min. The sectional scans with MitoTracker red dye, those with MitoTracker red plus MitoTracker green dyes and those with MitoTracker red plus SYTO green dyes were obtained using computer-assisted confocal fluorescent microscopy (Fluoview FV300, Olympus, Tokyo) for analysis of the internal cellular structure.

2.6. Two color flow cytometry

After adding 20 nM MitoTracker red and 1 μM SYTO green, the samples were left standing for 15 min. The samples were examined with a flow cytometer (Epics Elite ESP, Beckman Coulter Inc., USA). The MitoTracker red dying was performed under non-saturating condition. False positives induced by the other spectrum band in two colors were detected using a negative control, and single labeling with MitoTracker red and SYTO green. Total cell counts of the mitochondrial cells or the cybrids were around 4000–8000.

3. Results

3.1. Generation of floating cells

To investigate the role of a pathogenic point mutation at nt 9176 (T9176C) of the mitochondrial genome, we constructed cybrid cell lines by fusing HeLa cells containing no mtDNA with platelets from healthy controls and patients with Leigh syndrome. The resultant cybrid cell lines were cloned (five control and 41 T9176C mutation cell lines). Cell line #1 was obtained from an older sister of a patient with Leigh syndrome who had the T9176C mutation. Cell line #2 was from the younger brother of a Leigh syndrome patient with the T9176 C mutation. Cell line #3 was from the controls. The cybrids initially showed an adherent form, but with continuing proliferation, new overlying cells began to grow over the adherent cells. As overgrowth proceeded, the overlying cells separated from the adherent cells and floated in the medium. The floating cells derived from the cybrid cell lines were collected and cultured in fresh DMEM medium supplemented with 10% FBS at 37 °C in a humidified gas mixture containing 8% CO_2. These floating cells have continuously increased under the same conditions for 1.5 years, with a doubling time of approximately 1 month.

3.2. Analysis of mtDNA of floating cells

To examine whether the floating cells did indeed originate from the cybrid cells that had been obtained by fusing platelets and Rho^0 HeLa cells, we used PCR–RFLP analysis to detect the T9176C mutation. The floating cells originating from the cybrids with the T9176C mutation have the mutation as shown in Fig. 1. However, the other floating cells originating from the control platelet-fused cybrids have the wild type mtDNA at nt 9176 (Fig. 1). The floating cells and their original cybrid cells were confirmed to have mtDNA derived from the platelets of the patient and control.

3.3. Characteristics of floating cells

The floating cells were not adherent, but rather

Fig. 1. Restriction fragment length analysis of the T9176C mutation in mitochondrial cells. In the presence of this mutation, the 178-bp amplified fragment was cut by ScrfI into fragments sized 151 and 27 bp (27 bp fragment not shown here), whereas wild type mtDNA remained uncut. Lanes 1–10 show the 151-bp fragment harboring the T9176C mutation, while lane 11 shows the wild type 178 bp fragment. Lanes 1–5 represent cell line #1 derived from the platelets of the older sister of a Leigh syndrome patient with the T9176C mutation. Lanes 6–10 represent cell line #2 derived from the platelets of the younger brother of a Leigh syndrome patient with the T9176C mutation. Lane 11 represents cell line #3 (control). Lane M is a size marker of ψ174/Hind III.

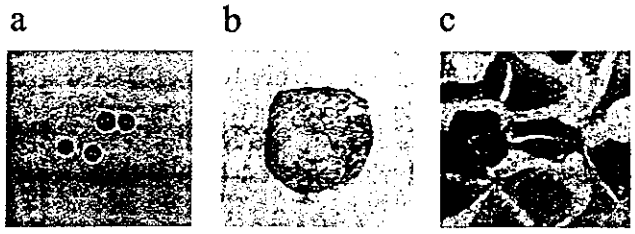

Fig. 2. The microscopic features of the floating cells derived from cell line #2 are shown. (a,b) The mitochondrial cells lack nuclei as shown by hematoxylin–eosin staining ((a) 50 × magnification, (b) 100 × magnification). The hematoxylin–eosin stained cytosol had a homogeneous eosin color, with no hematoxylin staining. (c) The positive control shows nuclei of the original cybrid cells stained with hematoxylin–eosin (100 × magnification).

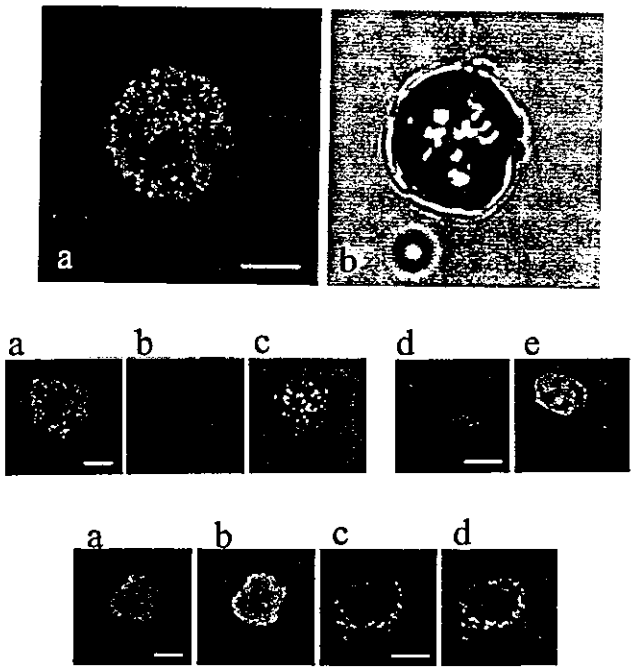

Fig. 3. Confocal fluorescence microscopic analysis of the floating cells and the original cybrids. (3-1) The wild type floating cells contained mitochondrial membrane activity as shown by MitoTracker red fluorescent dye. (60 × magnification). (a) The red granular particles are distributed throughout the cells. The shape and size are identical to mitochondria of the cybrids. (b) Light microscopy revealed the floating cells to be with rough membranous surface. Scale bar = 5 μm. (3-2) Mitochondria of wild type floating cells showed similar membrane specificity with dyes selective to the mitochondria of wild type cybrids (100 × magnification). (a) The wild type floating cells showed red granular particles when labeled with MitoTracker red, which is specific to mitochondrial membrane potential. (b) The wild type floating cells showed granular green staining when labeled with MitoTracker green, which is also mitochondrion-selective but membrane potential independent dye. (c,d) The mitochondria of the wild type cybrids showed granular red and green particles surrounding the nucleus, labeled with MitoTracker red dye (c), and MitoTracker green (d). Scale bar = 10 μm. (3-3) The floating cells lack nuclear structure and nuclear DNA, as shown by staining with MitoTracker red, and SYTO green dyes (100 × magnification) (a) The floating cells labeled with MitoTracker red revealed granular red particles. (b) The floating cells were negative for SYTO green staining. (c) Light microscopy revealed a membranous surface on the floating cells. (d) The mitochondria of the wild type cybrids showed granular red staining surrounding the nucleus, when labeled with MitoTracker red dye. (e) The nucleus of the wild type cybrids stained green when labeled with SYTO green. Scale bar = 10 μm.

formed loose aggregates. On microscopic examination, the cell surface had a rough membranous structure (Figs. 2b and 3-1c). The hematoxylin–eosin stained cells had a homogeneous eosin color, but surprisingly there was no hematoxylin staining suggesting the absence of a nucleus (Fig. 2a,b). In contrast, the original cybrid cells were revealed to have nuclei by hematoxylin staining (Fig. 2c). These results suggest that most of the floating cells lack nuclear structure and nuclear DNA.

3.4. Confocal fluorescence assays

MitoTracker CTX-Ros (hereafter referred to as MitoTracker red) detects mitochondrion-specific mitochondrial membrane potential. The floating cells were labeled with MitoTracker and observed with confocal fluorescence microscopy. As shown in Fig. 3-1a, granular particles were distributed in the cells. The shape and size were identical to those of the mitochondria of the cybrids (Fig. 3-2c,d). The MitoTracker green dye also labels mitochondria specifically regardless of mitochondrial membrane potential. Confocal fluorescence microscopy showed the floating cells to be positively stained with both MitoTracker red and MitoTracker green (Fig. 3-2a,b). The mitochondria of the wild type cybrids showed granular red and green stains surrounding the nucleus, labeled with MitoTracker red and MitoTracker green dyes (Fig. 3-2c,d). The positive MitoTracker green area was wider than that of MitoTracker red in both the floating cells and the cybrids (Fig. 3-2).

A fluorescent dye, SYTO green, stains nuclear DNA by penetrating membranes in living cells. We labeled the floating cells stained with MitoTracker red and SYTO green dyes. Confocal fluorescence microscopy showed positive MitoTracker red staining, while that of SYTO green was negative (Fig. 3-3a, b), and the original cybrids were stained with both MitoTracker red and SYTO green (Fig. 3-3d,e). These observations strongly suggested that most of the floating cells possessed mitochondrial membrane potential, but lacked nuclear structure and nuclear DNA. Thus, we designated these floating cells as mitochondrial cells. MitoTracker red and MitoTracker green strongly stained the surrounding area, but only weakly stained the central area, where nucleic acid staining was negative, in mitochondrial cells (Fig. 3-2c,d,3-3a,b). These findings suggest that mitochondria are not evenly distributed in the mitochondrial cells and that a non-staining substance is present in the central area; this may be an organelle other than mitochondria or nuclei, or some liquid as matrix in mitochondria or the cellular cytosol.

3.5. Flow cytometry of mitochondrial cells with SYTO green and MitoTracker

The MitoTracker red and SYTO green staining is shown in Fig. 4-1. The areas were divided into four parts depending on positive or negative SYTO green and MitoTracker red staining. We found 97.6% of T9176C mutation type mitochondrial cells and 99.6% of wild type mitochondrial cells to be in the SYTO green negative area. However, 92.4% of T9176C mutant type cybrids and 97.3% of wild type cybrids were in both SYTO green and MitoTracker red positive areas. These results indicate that the majority of mitochondrial cells lack a nucleus, while no more than a few percent of these cells contain a nucleus or nuclear DNA.

Using MitoTracker red, mitochondrial membrane potential was compared between mtDNA with the T9176C mutation and wild type mtDNA in the mitochondrial cells and cybrids (Fig. 4-2). The mitochondrial cells with the T9176C mutation had less active mitochondrial membranes than those with wild type mtDNA. The intensity of MitoTracker was 17.4 ± 20.4 (mean $\pm$ standard deviation) in the T9176C mutant type mitochondrial cells, and 37.8 ± 30.9 in the wild type cells. The result was comparable to the difference in staining between the cybrids with the T9176C mtDNA mutation and those with wild type mtDNA. The intensity was 43.5 ± 79.9 in the mutation cybrids and 101.6 ± 71.7 in the wild type cells. The cybrids with the T9176C mutation also had less active mitochondria than those with wild type mtDNA. The intensity of the mitochondrial cells was lower than that of the cybrid cells, because the mitochondrial cells were smaller than the cybrids. This observation indicated that the T9176C mtDNA mutation decreases in mitochondrial membrane potential regardless of the existence of a nucleus.

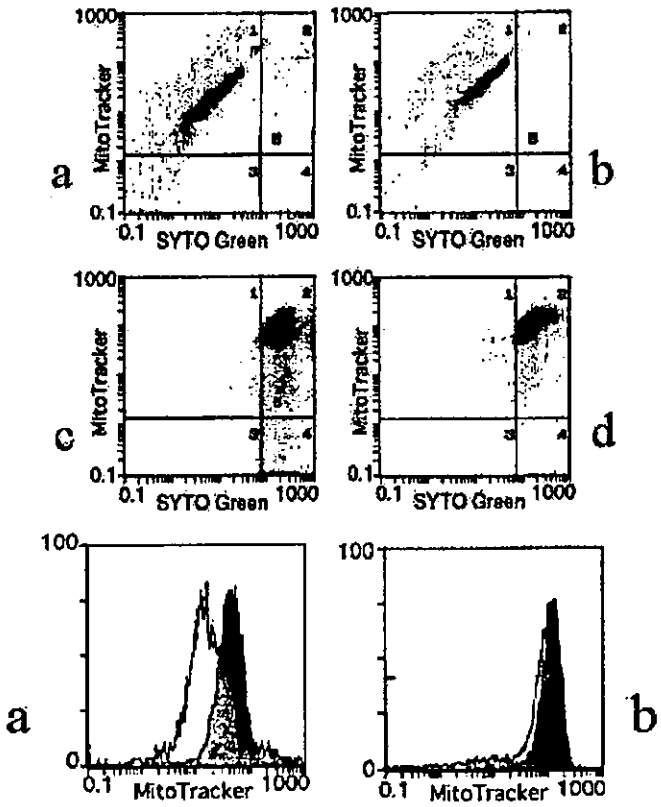

Fig. 4. Flow cytometry in mitochondrial cells and original cybrids with SYTO green and MitoTracker red dyes. (a) Mitochondrial mutation T9176C type cells. (b) Mitochondrial wild type cells. (c) Mitochondrial mutation T9176C type cybrids. (d) Wild type cybrids. (4-1) The mitochondrial cells lack a nucleus or most nuclear DNA, but still have mitochondrial membrane potential as shown by staining with both MitoTracker red and SYTO green. The areas were divided into four groups based on positive or negative SYTO green and MitoTracker red staining. The standard for positive vs. negative was defined by comparison with a negative control and single label staining of the cybrids. (a) T9176C mutation type mitochondrial cells (97.6%) and (b) wild type mitochondrial cells (99.6%) were in the SYTO green negative area, consisting of areas 1 and 3 in each figure. (c) T9176C mutant type cybrids (92.4%) and (d) wild type cybrids (97.3%) were in both SYTO green and MitoTracker red positive areas, represented in area 2. (4-2) The mitochondrial cells with T9176C mutation mtDNA had less active mitochondrial membranes than those with wild type mtDNA as evaluated by MitoTracker red staining. The cybrids showed similar results. (a) The left open curve represents the intensity of the mitochondrial cells with the mutation. The right closed black curve represents that of the wild type mitochondrial cells. (b) The left open curve shows the intensity of cybrids with the mutation. The right closed black curve shows that of the wild type cybrids.

4. Discussion

Our results are surprising as this type of cell, with active mitochondria but without a nucleus, has not previously been reported. We would like to emphasize that these mitochondrial cells have been obtained repeatedly from cybrids, with and without the pathogenic mutation. It was not an isolated or unusual event. Since only a small percentage of cells in the population contains a nucleus, it is likely that the mitochondrial cells were generated from progenitor cells with nuclear DNA and maintained for a considerable time. However, the nuclear DNA of the parental progenitor cells must have been derived from HeLa cells. An unknown signal may stimulate the HeLa nucleus from the cytosol or mitochondria.

These mitochondrial cells are anticipated to be useful for investigating how the nucleus is lost, the signaling pathways involved and how mitochondria are maintained. In addition, they may be used for investigating the role of mutant mitochondria as the effect of nuclear background can be excluded in these cybrids.

Acknowledgements

We thank the patients and staff at Department of Pediatrics, TWMU for their cooperation, and Y. Kaneko, R. Takahashi and Y. Kawakita for their technical assistance. This work was supported in part by Morinaga Foundation (K.N.) and the Japan Epilepsy Research Foundation (K.N.).

References

Anderson, S., Bankier, A.T., Barrell, B.G., et al., 1981. Sequence and organization of the human mitochondrial genome. Nature 290, 457–465.

Campos, Y., Martin, M.A., Rubio, J.C., et al., 1997. Leigh syndrome associated with the T9176C mutation in the ATPase 6 gene of mitochondrial DNA. Neurology 49, 595–597.

Chomyn, A., Martinuzzi, A., Yoneda, M., et al., 1992. MELAS mutation in mtDNA binding site for transcription termination factor causes defects in protein synthesis and in respiration but no change in levels of upstream and downstream mature transcripts. Proc. Natl Acad. Sci. USA 89, 4221–4225.

Chomyn, A., Lai, S.T., Shakeley, R., Bresolin, N., Scarlato, G., Attardi, G., 1994. Platelet-mediated transformation of mtDNA-less human cells: analysis of phenotypic variability among clones from normal individuals and complementation behavior of the $tRNA^{Lys}$ mutation causing myoclonic epilepsy and ragged red fibers. Am. J. Hum. Genet. 34, 966–974.

Dunbar, D.R., Moonie, P.A., Zeviani, M., Holt, I.J., 1996. Complex I deficiency is associated with 3243G:C mitochondrial DNA in osteosarcoma cell cybrids. Hum. Mol. Genet. 5, 123–129.

Frey, T., 1995. Nucleic acid dyes for detection of apoptosis in living cells. Cytometry 21, 265–274.

Gu, M., Cooper, J.M., Taanman, J.W., Schapira, A.H., 1998. Mitochondrial DNA transmission of the mitochondrial defect in Parkinson's disease. Ann. Neurol. 44, 177–186.

Hollinshead, M., Sanderson, J., Vaux, D.J., 1997. Anti-biotin antibodies offer superior organelle-specific labeling of mitochondria over avidin or streptavidin. J. Histochem. Cytochem. 45, 1053–1057.

King, M.P., Attardi, G., 1989. Human cells lacking mtDNA: repopulation with exogenous mitochondria by complementation. Science 264, 500–503.

Ligon, L.A., Steward, O., 2000. Movement of mitochondria in the axons and dendrites of cultured hippocampal neurons. J. Comp. Neurol. 427, 340–350.

Makino, M., Horai, S., Goto, Y.-I., Nonaka, I., 1998. Confirmation that T-to-C mutation at 9176 in mitochondrial DNA is an additional candidate mutation for Leigh's syndrome. Neuromuscul. Disord. 8, 149–151.

Nakano, K., Nakayama, T., Sasaki, K., Osawa, M., 1999. Clinical characteristics of acute aggravation in Leigh syndrome with T9176C mutation of mitochondrial ATPase 6 gene. Japanese Journal for Inherited Metabolic Diseases, 15, 217 pp. (in Japanese)

Ohta, S., 1986. Production of monoclonal antibody with in vitro immunization. Saiboukogaku (Jpn. Cell Technol.) 5, 160–165.(in Japanese).

Sambrook, J., Fritsch, E.F., Maniatis, T., 1989. Isolation of DNA from mammalian cells. Protocol I, II, III. Molecular Cloning, a Laboratory Manual, second ed., Cold Spring Harbor Laboratory, Cold Spring Harbor, NY, pp. 9.16–9.23.

Shults, C.W., Beal, M.F., Fontaine, D., Nakano, K., Haas, R.H., 1998. Absorption, tolerability, and effects on mitochondrial activity of oral coenzyme Q_{10} in Parkinson patients. Neurology 50, 793–795.

Thyagarajan, D., Shanske, S., Vazquez-Memije, M., De Vivo, D., DiMauro, S., 1995. A novel mitochondrial ATPase 6 point mutation in familial bilateral striatal necrosis. Ann. Neurol. 38, 468–472.

臨床編 II

ミトコンドリア病(狭義)

心ブロック

Heart block

中野和俊　中山智博　佐々木香織

Key words: 心ブロック，Kearns-Sayre症候群，房室ブロック，動物モデル，ミトコンドリアDNAの欠失

1. ミトコンドリア病における心ブロック，心伝導障害の頻度

心ブロックを含む心伝導障害はミトコンドリア脳筋症全体でみた場合，頻度は決して高くない．しかし，ミトコンドリア脳筋症の種々の臨床型で認められ，しばしば進行性であり，突然死などの重要な死亡原因になるという点から重要である．ミトコンドリア脳筋症はKearns-Sayre症候群(KSS)，mitochondrial encephalomyopathy, lactic acidosis and stroke-like episodes(MELAS)，myoclonus epilepsy with ragged red fibers(MERRF)をはじめとして，Leber's hereditary optic neuropathy(LHON)など種々の臨床型がある．

これまで最も多く心伝導障害合併が報告されている臨床型は，KSSを中核とする慢性進行性外眼筋麻痺(chronic progressive external ophthalmoplegia: CPEO)である．阿南らの検討では，CPEOの33％で心電図異常が認められた[1]．MELASにおいては，小澤らは14％の心伝導障害を報告し[2]，阿南らは6例中4例(66％)の心電図異常を指摘している[1]．MERRFにおいては，福原の集計では23例中1例(4％)に心伝導障害が認められている[3]．以下，各ミトコンドリア脳筋症臨床型と心伝導障害について述べる．

2. 各疾患と心伝導障害

a. CPEO，KSSと心伝導障害

KSSは，慢性進行性の外眼筋麻痺を主症状とする慢性進行性外眼筋麻痺に網膜色素変性，心伝導障害を加えた3主徴を特徴とする．Berenbergらは，自験例5例を含む35例を集計し，KSSでは心臓障害によりAdams-Stokes発作が29％，心停止が6％，うっ血性心不全が11％にみられ，合計46％に達すると報告している[4]．KSSにおける心伝導障害は完全房室ブロック[5]，脚ブロックが初期より報告され，Robertsらの自験例2例を含む19例の集計[6]では，完全房室ブロックが2例(観察中に更に2例)，右脚ブロックと左軸偏位が16例，Mobitz IIの2度房室ブロックが4例，PR短縮が2例にみられたと報告している．

このほかにKSSの心伝導障害には1度房室ブロック[7]，左前枝ブロック，左後枝ブロック，心室内伝導障害が多い．His束心電図による検討[8]では，心房His束間は正常でHis束間心室間(H-V)の延長が認められH-Vブロックが明らかになった(図1)．病理所見と考え合わせると，この結果はKSSの多くがHis束-Purkinje系の障害を有することを示唆するものである．しかし，洞結節の障害を示唆する洞性不整脈の報告もあ

Kazutoshi Nakano, Tomohiro Nakayama, Kaori Sasaki: Department of Pediatrics, Tokyo Women's Medical University　東京女子医科大学小児科

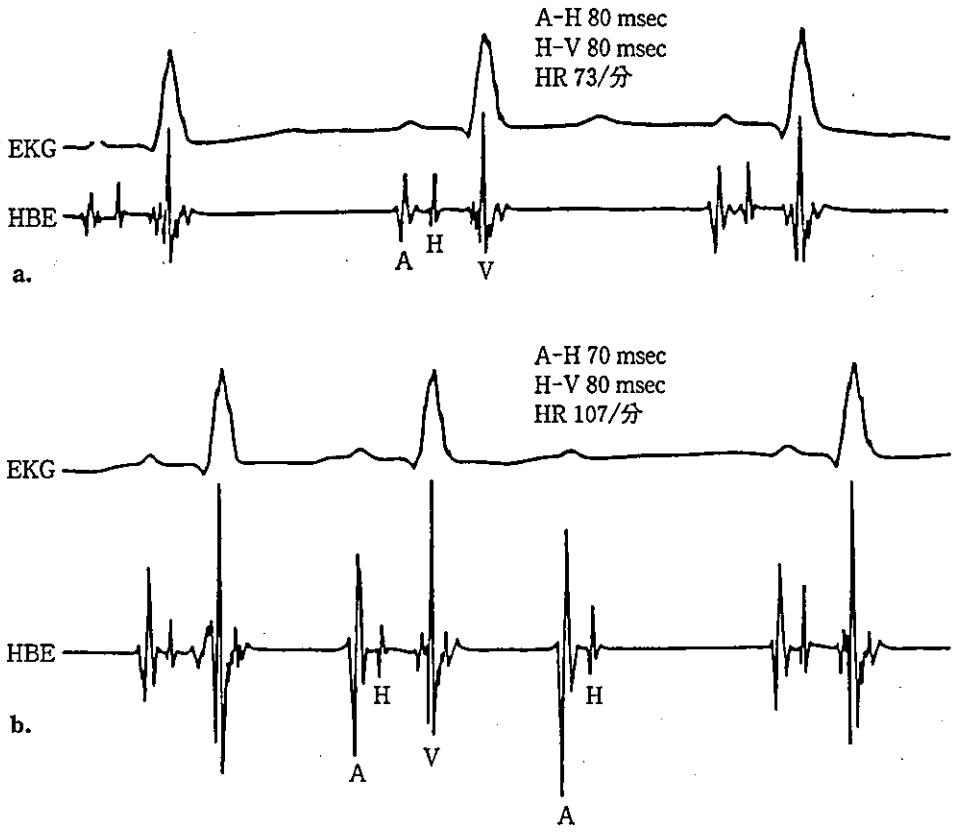

図1 Kearns-Sayre 症候群(KSS)における心電図，His 束心電図同時記録
Aは心房性脱分極．Hは His 棘波．Vは心室性脱分極．aは負荷のない状態．bはアトロピンを負荷し，脈拍が107/分に上昇した状態．A-H伝導時間は短縮しているが，H-V伝導時間は変わらない．2：1 Mobitz II型房室ブロックがあり，His 束より末梢のブロックを呈している．

る[9]．

阿南は，KSSの1例で13歳時に二枝ブロック(左脚前枝ブロック，完全右脚ブロック)と Mobitz IIの2度房室ブロックを呈し，15歳時に完全房室ブロックとなった例を呈示している．このように多くの例では脚ブロックから始まり，進行性に完全房室ブロックとなる．心伝導障害発現の平均年齢は17歳で[6]，10-20歳代で完全房室ブロックになる例が多いが，まれに年長者でみられる場合がある．

一般に右脚ブロックと左軸偏位は男性に多く，発生頻度は0.35％で予後は良好であり，人工ペースメーカー植え込みによる予防の対象にはならない．しかし，KSSにおいては虚血性心疾患よりも高率に完全房室ブロックに移行することが知られており，更に，その死亡率は20％に及ぶ．このため，突然死予防のため KSS は人工ペースメーカー植え込みの対象となる．人工ペースメーカー植え込みの適応基準として，2脚ブロック，H-Vブロックが提唱されている．

KSSの心ブロックの病態はいまだ明らかではないが，Gallastegui ら[10]は，左室駆出率の低下があり不整脈死した1例と心不全死した1例の計2例の剖検例を報告しており，心筋・刺激伝導系の変性，線維化，脂肪浸潤などを認めている．一方，QT延長症候群の洞結節で apoptosis の電顕像がとらえられており，ミトコンドリアを介した apoptosis などの細胞死のメカニズムが病態に関与していると推測される．

KSSの心ブロックの治療に coenzyme Q_{10} が有効であった報告がある[7]．coenzyme Q_{10} はミトコンドリア電子伝達系の基質であるが，無効の報告もあり同一病型であっても病期などにより薬の有効性が変わってくる可能性があると思

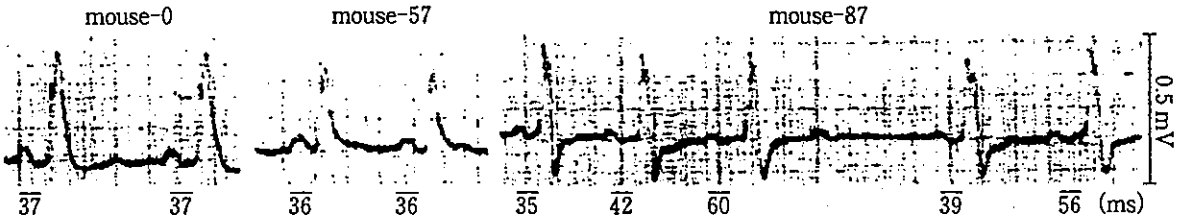

図2 CPEO/KSSのモデルとなり得る4696bp欠失(ΔmtDNA4696)mouseの心電図の変化
mouse-57および-87心筋のΔmtDNA4696変異率はそれぞれ58%，88%であった．mouse-87のみPQ間隔が延長し，Wenckebach型房室ブロックを示した．mouse-57の心筋cytochrome c oxidase(COX)染色はすべて正常陽性であるのに対し，mouse-87は陽性と陰性に染まる細胞が混在した．更に，COX染色電子顕微鏡で単一細胞内では，COX陽性かCOX陰性ミトコンドリアのいずれかでCOX陽性とCOX陰性ミトコンドリアが同時に存在しない．
(文献[15]より著者の承諾を得て引用)

われる．

b. MELASと心伝導障害

MELASは脳卒中様症状を主体とする臨床型である．MELASで心電図上，心室性期外収縮，上室性期外収縮，Wolff-Parkinson-White(WPW)症候群が認められるのみの比較的軽症の心伝導障害の報告がある一方，稲森ら[11]は，1度房室ブロックおよび不完全左脚ブロックから洞不全症候群に移行したミトコンドリアDNA A3243G変異を有する1例を報告している．この症例は糖尿病歴があり当初，心不全，高血圧に対し利尿剤などで治療していたところ洞不全症候群となり永久ペースメーカー植え込み術を行った．MELASは心疾患では心筋症が注目され，心伝導障害は比較的軽症と考えられてきたが，心ブロックを合併する場合は特に注意を要する．

c. MERRFと心伝導障害

MERRFはミオクローヌスてんかん，小脳症状，筋萎縮を主症状とする臨床型である．MERRFでは23例中1例の心伝導障害の報告はあるが，重篤例はなく心ブロックの報告はない．しかし，著者らはWPW症候群を5例中2例に経験しており，心ブロックへの移行の有無について症例を蓄積する必要がある．

d. その他のミトコンドリア脳筋症と心伝導障害

KSS，MELAS，MERRF以外のミトコンドリア脳筋症では，LHONでWPW症候群合併の報告がある[12]．更に，histiocytoidまたはoncocytic fetal mitochondrial cardiomyopathyとして上室性，心室性頻脈，心停止などの致命的な不整脈を伴い，2歳までに死亡する疾患が報告されている[13]．この疾患では心筋ミトコンドリア電子伝達系で複合体IIIの欠損が報告されているが，遺伝子変異は明らかになっていない．また，心伝導障害の一つにQT延長症候群があるが，Matsuokaら[14]は，QT延長症候群にミトコンドリアDNAのND1におけるT3394C変異が認められ，同変異のサイブリッド細胞において電子伝達系酵素複合体I活性低下，酸素消費の低下を認め，QT延長の原因[13]となっていると報告している．

3. ミトコンドリア遺伝子(mtDNA)変異と心ブロック

心ブロックを呈するミトコンドリア病の主な臨床型はCPEO/KSSである．多くのCPEO/KSS遺伝子変異はmtDNAの単一大欠失を示し，欠失の長さは1-10kbまで様々であるが，約1/3はcommon deletionと呼ばれ，4,988 base pair(bp)(mtDNAは16,569bp)で両端には13bpの繰り返し配列があり，これが欠失発生機構に関連している可能性がある．現在のところ，報告されている症例は孤発性である．

最近，Hayashiら[15]により，母系遺伝のmtDNA変異をもつ動物モデルが作り出された．その変異はCPEO/KSSのモデルとなり得る4696bp欠失(ΔmtDNA4696)である．彼らはこの動物モデルにおいて，心筋を含む各組織のすべてのミト

コンドリアにおいてΔmtDNA4696変異の割合が優位でなければcytochrome c oxidase(COX)活性は正常であり，心ブロックなどの症状は発現しないことを明らかにした(図2)．更に，単一細胞内ではCOX陽性とCOX陰性ミトコンドリアが同時には存在しないことから，ミトコンドリアが互いに融合し相補的に機能していることを裏付けた．この動物モデルの開発により，心ブロックの解明が更に進み，ミトコンドリア遺伝子治療の可能性が開かれることが期待される．

謝辞

本論文を御校閲いただいた大澤真木子教授に深謝いたします．

■文　献

1) 阿南隆一郎：ミトコンドリア病における心病変の臨床的検討．医学研究　61: 49-61, 1993.
2) 小澤真津子，後藤雄一：MELAS(mitochondrial myopathy, encephalopathy, lactic acidosis, and stroke-like episodes)．最新医学　50: 1292-1296, 1995.
3) 福原信義：ミトコンドリア脳筋症の臨床．神経進歩　31: 604-617, 1987.
4) Berenberg RA, et al: Lumping or splitting? 'Ophthalmoplegia-plus' or Kearns-Sayre syndrome? Ann Neurol　1: 37-54, 1977.
5) Kearns TP, Sayre GP: Retinitis pigmentosa, external ophthalmoplegia and complete heart block. Arch Ophthalmol　60: 280-289, 1958.
6) Roberts NK, et al: Cardiac conduction in the Kearns-Sayre syndrome (a neuromuscular disorder associated with progressive external ophthalmoplegia and pigmentary retinopathy): report of 2 cases and review of 17 published cases. Am J Cardiol　44: 1396-1400, 1979.
7) Ogasahara S, et al: Improvement of abnormal pyruvate metabolism and cardiac conduction defect with coenzyme Q10 in Kearns-Sayre syndrome. Neurology　35: 372-377, 1985.
8) Morriss JH, et al: His bundle recording in progressive external ophthalmoplegia. J Pediatr　81: 1167-1170, 1972.
9) Ulicny KS, et al: Sinus dysrhythmia in Kearns-Sayre syndrome. Pace　17: 991-994, 1994.
10) Gallastegui J, et al: Cardiac involvement in the Kearns-Sayre syndrome. Am J Cardiol　60: 385-388, 1987.
11) 稲森正彦ほか：糖尿病を有し，心不全，洞不全症候群を呈したミトコンドリアtRNA$^{LEU(UUR)}$遺伝子の3243変異を伴ったミトコンドリア脳筋症の1例．J Cardiol　30: 341-347, 1997.
12) Nikoskelainen EK, et al: Pre-excitation syndrome in Leber's hereditary optic neuropathy. Lancet　344: 857-858, 1994.
13) Papadimitriou A, et al: Histiocytoid cardiomyopathy of infancy: deficiency of reducible cytochrome b in heart mitochondria. Pediatr Res　18: 1023-1028, 1984.
14) Matsuoka R, et al: A mitochondrial DNA mutation cosegregates with the pathophysiological U waves. Biochem Biophys Res Commun　257: 228-233, 1999.
15) Nakada K, et al: Inter-mitochondrial complementation: mitochondria-specific system preventing mice from expression of disease phenotypes by mutant mtDNA. Nat Med　7: 934-940, 2001.

綜説

MELASにおける脳卒中様発作と臨床

松崎 美保子* 中野 和俊* 大澤 真木子*

要旨

8例のMELAS自験例を示し，発作症状について整理を試みた．卒中様発作の主症状は，けいれん，頭痛・嘔吐，視覚症状，一過性運動麻痺であった．けいれん主体発作では，片頭痛様頭痛，視覚症状を伴う点で頭痛・嘔吐発作と類似していた．卒中様発作時脳波は，後側頭葉～後頭葉に徐波バースト(徐波が発作性に持続)，突発性高振幅徐波に多棘波が重畳したバーストを呈した．脳画像では，後頭葉，前頭葉の皮質および皮質下，小脳半球に病変の好発部位を示した．卒中様発作はmicroangiopathyに起因し，発作の反復が不可逆性脳障害を惹起すると推測された．機序として，嫌気性解糖による局所の高乳酸アシドーシスが考えられている．

はじめに

ミトコンドリアは，赤血球以外の全身の細胞に存在する細胞小器官である．糖，アミノ酸，脂肪酸などの基質を，生体への最終的なエネルギー供給源であるATPへと変換する働きをする．ミトコンドリア内には種々の代謝経路があるが，エネルギー代謝には，電子伝達系，TCA回路，脂質代謝系，アミノ酸代謝系などが関係する．電子伝達系は，主としてTCA回路から電子をもらい受けることにより還元エネルギーを得る．これによりH^+がミトコンドリア内膜から排出され電気化学的プロトン勾配ができ，この勾配を用いて最終的にATPを生成する代謝系である．

ミトコンドリア内には，核のDNAとは別に独自のゲノムであるミトコンドリア遺伝子(mtDNA)が存在し，それによりコードされる蛋白質は核DNAにコードされる蛋白質とともに，ミトコンドリア内膜で集合して酵素複合体を形成する．mtDNAは，mRNA, rRNA, tRNAの遺伝子をもち，ATP合成に必要な呼吸酵素複合体I，III，IV，Vのサブユニット蛋白質の一部に転写，翻訳される．ミトコンドリア脳筋症の患者では，細胞内（おそらくはミトコンドリア内）には変異型DNAと野生型DNAが共存している．変異型が占める割合がある一定の閾値以上になると，ミトコンドリア呼吸酵素の機能不全によるエネルギー産生低下が生じ，エネルギー依存度が高い中枢神経系，骨格筋，心筋において障害がでやすい[1]（閾値理論）．

1984年，Pavlakisら[2]が反復する脳卒中様発作と高乳酸血症を特徴とする進行性のミトコンドリア脳筋症の一型をMELASとして提唱し

* Mihoko MATSUZAKI et al. 東京女子医科大学小児科
[連絡先] 〒162-8666 東京都新宿区河田町8-1 東京女子医科大学小児科

た．ミトコンドリア機能異常，形態異常，mtDNA の $tRNA^{Leu(UUR)}$ 領域の 3243 の A から G への点変異および 3271 の T から C への点変異と強い関連があり[3)4)]，母系遺伝する．同部位の点変異は，感音性難聴を伴う母系遺伝の糖尿病患者においても関連がある[5)~7)]．同一の遺伝子異常が，なぜ異なる臨床症状を呈するのか不明である．

I．MELAS の診断と治療

発症前は正常発達．反復する頭痛・嘔吐発作，反復する卒中様発作（閃光，暗点，半盲，全盲などの視覚症状や片麻痺などの局所神経症状を伴い，数日片頭痛が遷延），けいれん，けいれん後の一過性片麻痺，左右の反復する片麻痺，半盲，筋力低下，進行性知的退行，感音性難聴，低身長などの症状を呈する．血中高乳酸性アシドーシス，髄液中の乳酸/ピルビン酸比が 20 以上，筋生検で赤色ぼろ線維（ragged-red fiber：RRF）を認め，筋細胞，白血球，血小板で mtDNA 点変異を認めることを参考に診断する．

エネルギー産生異常に対してビタミン B 1，B 2 大量療法，ジクロロ酢酸，クレアチン療法などが補充療法[8)9)]として行われている．卒中様発作，けいれんの治療として，GABA 作動性ニューロンに作用するベンゾジアゼピン系化合物であり，大脳皮質の興奮性に抑制作用をもつミダゾラム静注[10)]，一酸化窒素の発生を促し血管拡張作用により卒中様発作改善効果を有する L-アルギニン療法[11)]が試みられている．

II．脳卒中様発作

数日続く激しい頭痛，嘔吐発作，意識障害，視覚症状が先行することがあり，けいれん後に一過性片麻痺を伴うことがある．脳病変は血管支配と異なり，脳梗塞とは異なる病態が示唆されてきた[12)]．自験した，筋症状で発症した 4 例，中枢神経症状で発症した 3 例，双方の症状で発症した 1 例のうち，代表例を提示し，発作症状につき考察する．

[症例 1]　女児[10)]

母は A 3243 G 点変異があり．兄は 21 トリソミー．本児は 3 歳まで正常発達後，易疲労性，体重減少が出現．4 歳 8 カ月，尿路感染症罹患時に発熱，筋力低下により一過性に立位不可．遺伝子診断で A 3243 G の変異を認め，MELAS と診断．5 歳 3 カ月以降，嘔吐，眼がチカチカするという視覚症状，意識障害を伴う脳卒中様発作が数回出現．7 歳 6 カ月ごろから意欲低下，ふらつき，色の識別不能，視力低下が出現．7 歳 7 カ月知的および運動能力退行が急速に進行し，歩行不可となり，錐体路徴候，皮質盲が出現，固定化した．

7 歳 9 カ月に頭部 MRI にて小脳と後頭葉に特定の脳血管支配領域に一致せず梗塞巣が出現．8 歳 10 カ月には嘔吐，発熱出現 14 時間後に全身間代性けいれん，9 歳 1 カ月には激しい頭痛・嘔吐発作，39°C の発熱，傾眠傾向を呈した．眼球一点凝視，酸素飽和度の低下を伴う意識障害のエピソードが群発した．MRI-T 2 画像で，左後側頭葉～後頭葉皮質に脳回に沿った高信号域を，両側・後側頭葉～後頭葉および右前頭葉の皮質下に側脳室に沿って多嚢胞状の高信号域を認めた（図 1）．意識消失発作は，ジアゼパム座剤 10 mg 投与では不変．ミダゾラムを 0.3 mg/kg 静注開始直後から意識清明となり 0.2 mg/kg/hr で持続投与した．脳波において，左後側頭葉～後頭葉領域に律動性徐波を認めた（図 2-左）．

9 歳 2 カ月，嘔吐・頭痛数時間後に左上肢の間代性けいれんが群発，脳波において右後側頭葉～後頭葉～頭頂に律動性徐波を認め（図 2-右），ミダゾラム 0.14 mg/kg 持続静注でいったん症

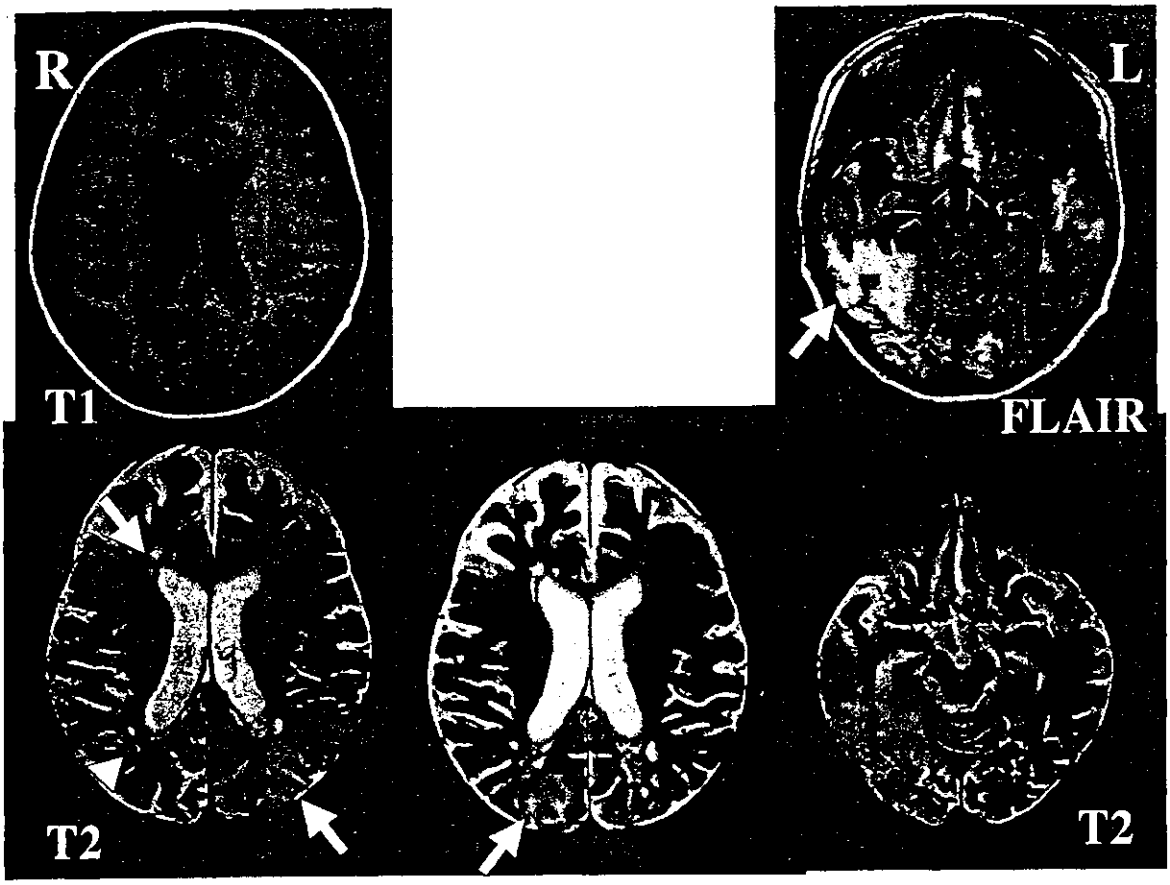

図1　症例1の頭部 MRI

9歳1カ月には，T2画像で，左後側頭葉～後頭葉皮質に高信号域を，両側・後側頭葉～後頭葉および右前頭葉皮質下に多嚢胞状の高信号域を示した．9歳2カ月，T2画像において右後頭葉に高信号域を示した．

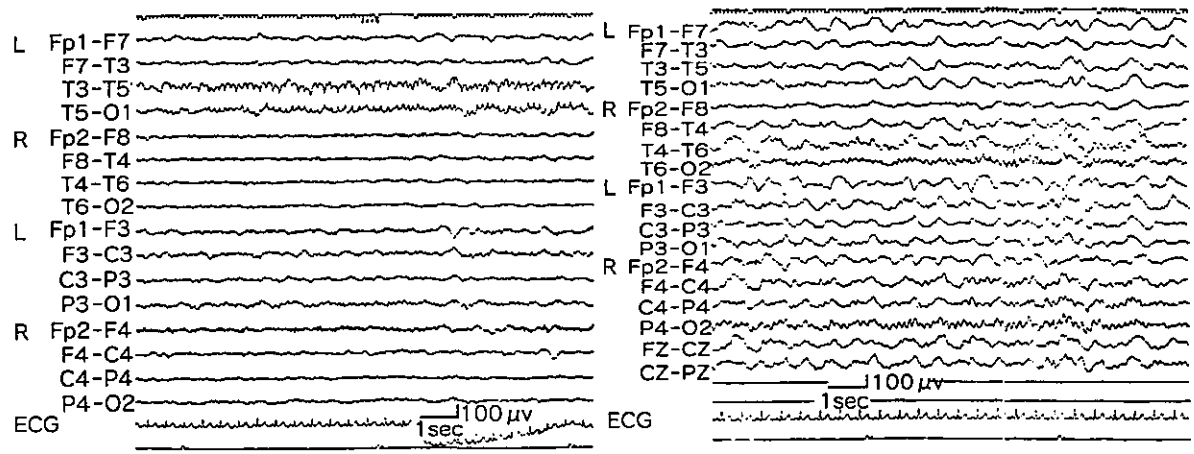

図2・ 症例1の脳波

左は9歳1カ月，意識障害を伴う頭痛・嘔吐発作時．右は9歳2カ月，左上肢の間代性けいれんを伴う卒中様発作時における，けいれん消失時の記録．各々，左後側頭葉～後頭葉，右後側頭葉～後頭葉～頭頂に 6～7 Hz 徐波バーストが認められた．1カ月の経過で，発作巣が変化した．

状は消失した．しかし9日後に左上肢の持続性部分てんかん(EPC)が出現，ミダゾラムを0.2 mg/kgに増量し約48時間後に頓挫した．MRI-T2画像で新たに右後頭葉に高信号域を認めた(図1)．ミダゾラム持続静注により，頭痛・嘔吐発作を認めるもけいれんには至らなかった．

9歳8カ月，38℃の発熱の翌日，不機嫌の状態が続いていた．誘因なく「恐い！恐い！」と叫び出し全身を震わせて母にしがみつき，意識が混濁した．頭痛を認めず．ミダゾラム0.25 mg/kgを静注し，数十秒後に意識清明，会話が可能となり，恐怖感が消失した．頭部MRIで新たに左側頭内側領域に新たな梗塞巣を認め，側頭葉症状と考えた．

9歳10カ月，睡眠中の下肢にミオクローヌス様のけいれん，10歳10カ月以降，上下肢のミオクローヌスに続いて，体幹・四肢を硬直，無言となる強直けいれんと考えられる発作が群発した．

[症例 2] 男児[13]

母と本人に，mtDNA A 3243 Gの点変異あり．正常発達であったが，3歳3カ月，微熱が1カ月続き，一過性に立位不可になった．他院で筋生検施行，MELASの診断．4歳6カ月，目が見えないという視覚異常に引き続き，嘔吐，意識障害を伴う卒中様発作が出現．4歳8カ月，意識障害を伴う嘔吐発作，脳波では両側の後側頭葉～後頭葉に高振幅徐波が，さらに左後頭葉に多棘波が重畳していた(図3)．5歳0カ月眼球偏位，顔面蒼白，嘔吐後に入眠．5歳1カ月反復する頭痛，左上肢・間代性けいれん．5歳6カ月からは右半身または左半身を移動しながら持続するEPCを呈するようになった．脳画像上，小脳半球，左右の後頭葉に梗塞巣が交互に出現し，半身けいれんまたは半身に留まるEPCが左，右，左，右と交互に現れた．6歳11カ月，拡張型心筋症による心不全で死亡．

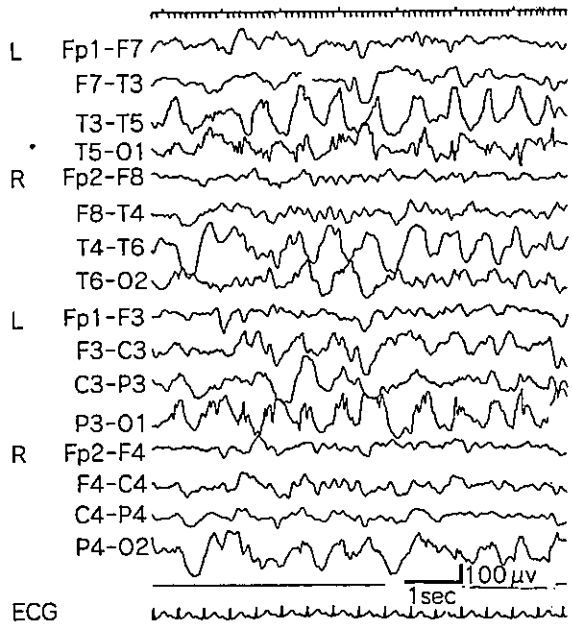

図3 症例2の脳波

4歳8カ月，嘔吐発作時の記録．両側の後側頭葉～後頭葉に1.5～2 Hzの不規則高振幅徐波が，さらに左後頭葉に多棘波が重畳している．

[症例 3] 女児

母方叔父は，35歳時突然死，心筋梗塞が疑われたが確証はない．生来健康．14歳0カ月から疲れやすくなった．14歳2カ月から頭痛を頻回に訴える．14歳6カ月，運動後に全身性強直性間代性けいれん．頭部CTと脳波で異常を認めず．14歳7カ月から集中力，学力が低下した．14歳10カ月，5分間の暗点，半月後には1分間の全身性強直性間代性けいれん，頭部CTでは正常所見．15歳2カ月，半日ほど目の奥がチカチカする感あり．翌日から頭痛，3～4病日にかけて嘔吐，応答は鈍いものの意識は清．4病日には黄斑回避を伴う右・同名半盲を認めた．脳波では，左後頭葉に高振幅徐波に多棘波が重畳した(図4)．23病日には改善．7病日の頭部CTで左後頭葉において低吸収域を認めた．高乳酸血症，筋生検でRRFを認めMELASと診断．退院後，転院．

[症例 4] 女児[10]

家族歴に特記すべきことなし．6歳まで正常発達．6歳よりときどき頭痛を訴え疲れやす

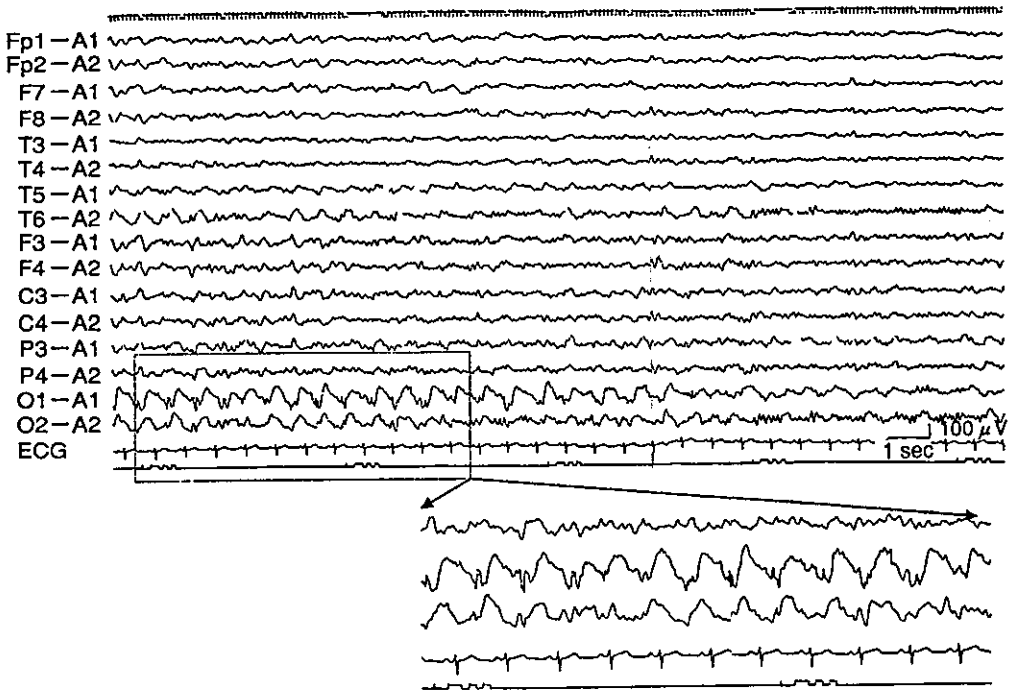

図4　症例3の脳波

15歳2カ月，頭痛・嘔吐発作による目の奥のチカチカ，頭痛後に右・同名半盲を呈したときの記録．左後頭葉に，一見すると不規則多棘徐波複合様ではあるが，一部は1.5 Hzの高振幅徐波に多棘波が重畳している．

かった．9歳9カ月，2日間の頭痛，嘔吐，半日後に発熱，目が見えないという視力障害が1日続いた．9歳11カ月，運動後より頻回嘔吐，頭痛，翌日から傾眠傾向，発熱．意識減損に一致して，脳波において左後頭葉が右側に先行して棘波バーストおよび高振幅徐波に多棘波が重畳した（図5）．ジアゼパム静注で発作波は一過性に消失，フェニトイン静注18 mg/kgで脳波所見，意識が改善し，目が見えないと訴えた．視覚誘発電位により皮質盲と診断．頭部MRIで異常を認めず．3病日に症状，誘発電位所見は改善した．髄液中の乳酸，ピルビン酸値上昇，筋生検でRRFを，mtDNA検索でA 3243 G点変異を認め，MELASと診断した．

10歳0カ月頭痛・嘔吐発作，10歳2カ月堪え難い頭痛，意識障害，眼瞼ミオクローヌスが反復出現した．発作時脳波は，左後頭葉に棘波バースト，右後頭葉に徐波バーストが出現した後，両側全般性・左右同期性高振幅徐波に多棘波が重畳し，発作波は突然終了した（図6）．キシロカイン2 mg/kg/hr，フェニトイン20 mg/kg静注無効．ミダゾラム0.3 mg/kg静注後，0.2 mg/kg/hr持続静注が有効，頭痛発作，脳波異常群発は消失した．頭部MRI-FLAIR像で左後頭部，脳回に沿って高信号域を認めた．

10歳4カ月，頭痛，嘔吐，羞明感が出現．後頭部に律動性徐波バーストを認めミダゾラム0.3 mg/kg静注にて脳波は改善，0.3 mg/kg/hr持続静注で頭痛は消失．10歳9カ月，眼痛，頭痛，嘔吐発作出現．2病日にMRI-T 2画像およびFLAIRで左後頭葉に高信号域．10歳10カ月頭痛が，11歳10カ月，4日間持続する頭痛，目がチカチカする発作が出現，同日MRI-T 2画像およびFLAIRにおいて右後頭葉に高信号域を示すも，12病日には改善．

11歳11カ月頭痛，目がチカチカ，左眼瞼優位のミオクローヌスに対して，ミダゾラム0.4 mg/kg/hrがやや有効であった．ビタミンC大

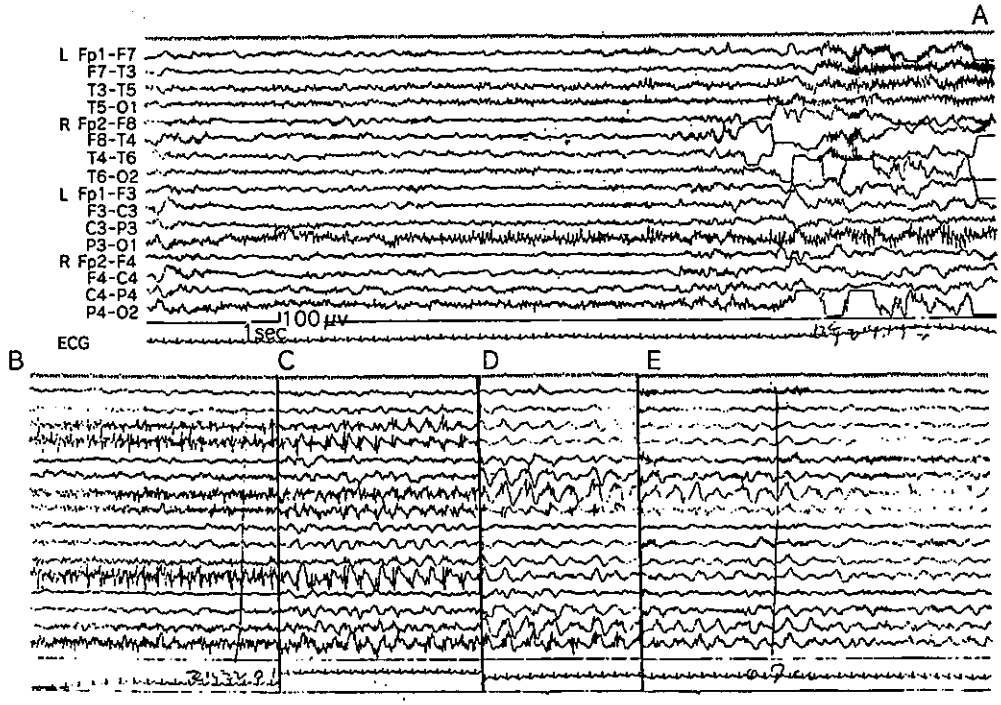

図5　症例4の9歳11カ月時の脳波

左後頭葉に棘波バーストが出現，(C) 以降，左後側頭葉～後頭葉において高振幅徐波に多棘波が重畳，(D)以降1Hz徐波に変容した．右半球の同部位にも遅れて同様の所見が得られた．A～B間7秒，A～C間43秒，A～D間144秒，A～E間164秒．

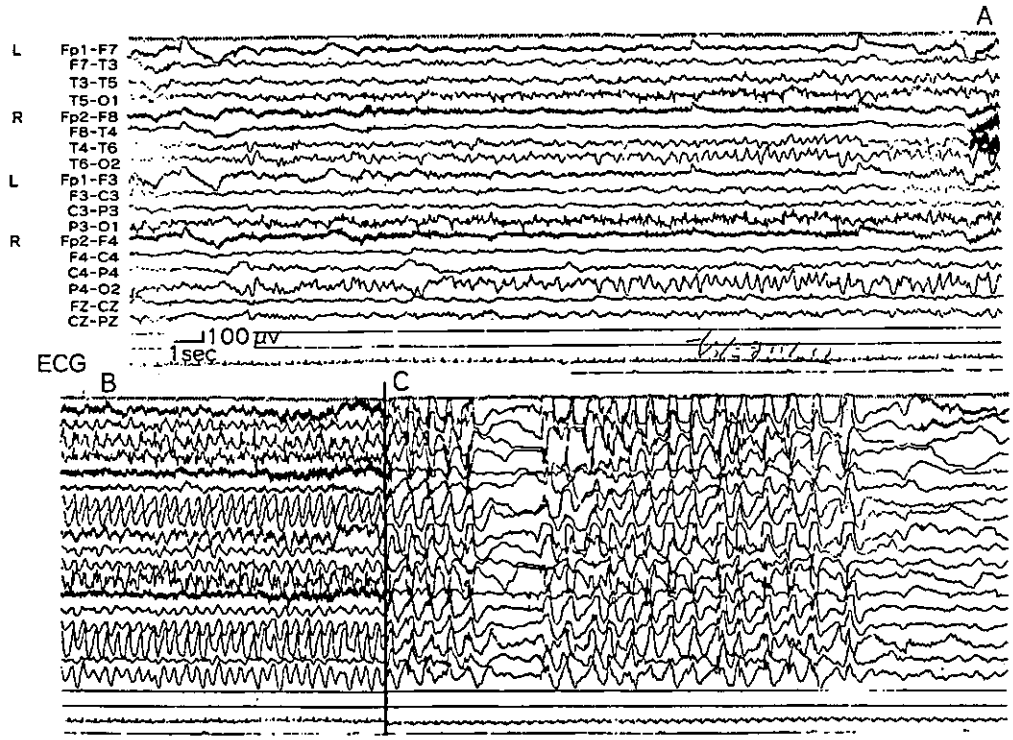

図6　症例4の10歳2カ月時の脳波

左後頭葉に多棘波バースト，対側後頭葉に徐波バーストが出現．全般性左右同期性高振幅徐波に全般性多棘波が重畳した．発作波は突然終了している．A～B間35秒，A～C間140秒．

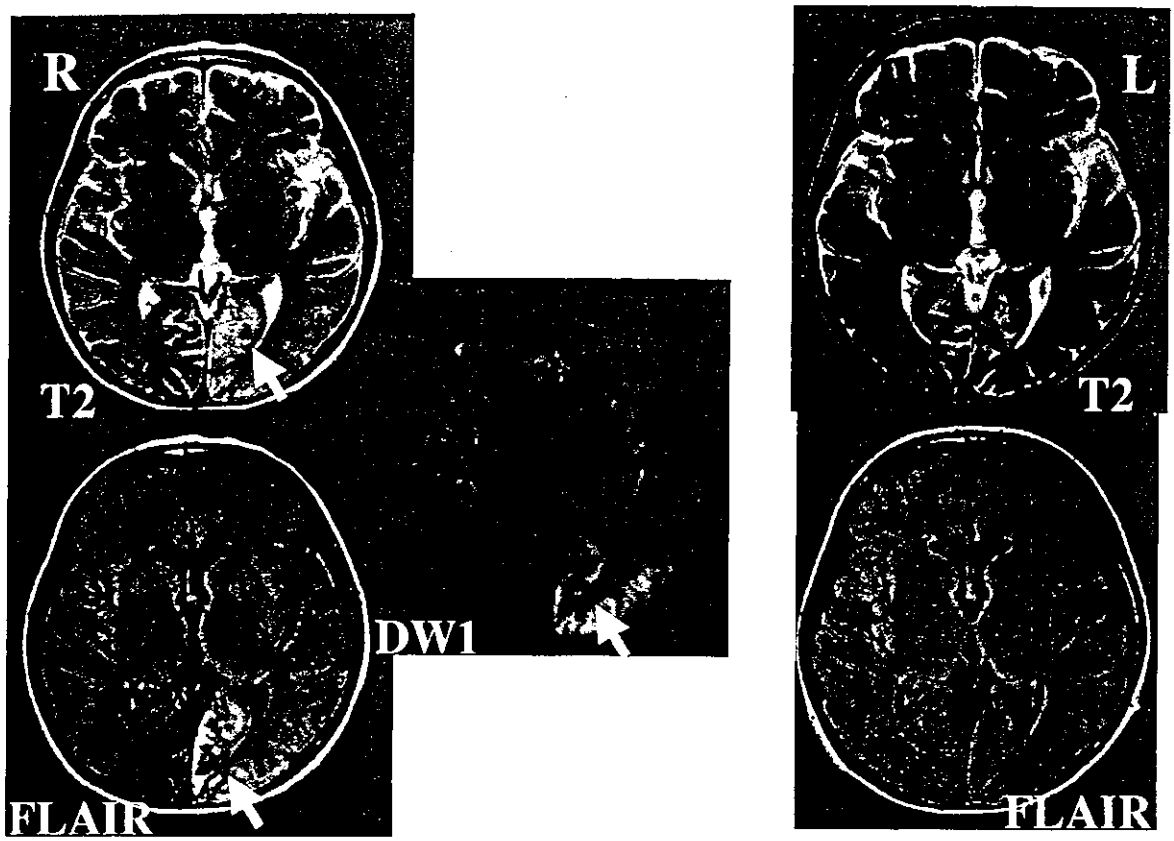

図7　症例4の11歳11カ月時のMRI

2病日において，MRI-T2画像，FLAIR，DW1で左後頭葉から頭頂葉にかけて認められた高信号域が，12病日には消失した．

量55 mg/kg静注，L-アルギニン療法500 mg/kg静注[11]が有効であった．2病日にMRI-T2画像，FLAIR，DW1で左後頭葉から頭頂葉にかけて高信号域を示し，12病日に行った追跡では病巣は消失していた(図7)．12歳0カ月，目のチカチカ，見えづらさ，頭痛が出現，ミダゾラム静注のみでは不変，L-アルギニン療法450 mg/kg静注，ジクロロ酢酸大量内服50 mg/kg/回を3回および半量で維持し，翌日には軽快した．

[症例5]　女児[13]

5歳5カ月までは，正常発達．5歳5カ月から6歳9カ月までに数回の無熱性・全身性強直性けいれんを起こし，6歳9カ月から8歳4カ月まで一過性，右および左の交代性片麻痺を4回繰り返し，7歳11カ月より右上肢の部分発作を認めた．高乳酸・ピルビン酸血症，筋生検上RRFを認め，MELASと診断した．mtDNA検索は未施行である．7歳11カ月ころより，てんかん性部分発作が，8歳4カ月ころより場面に不相応なてんかん性冷笑発作が出現，下肢優位の筋力低下，知的退行が徐々に進行，13歳5カ月現在，月単位の全身性けいれんが認められる．

III. 自験例における卒中様発作に関する分析

自験例での卒中様発作の主症状は，けいれん，頭痛・嘔吐，視覚症状，一過性運動麻痺であっ